AIP | Review of Scientific Instruments

A magnetic tunnel to shelter hyperpolarized fluids

Jonas Milani, Basile Vuichoud, Aurélien Bornet, Pascal Miéville, Roger Mottier, Sami Jannin, and Geoffrey Bodenhausen

Citation: Review of Scientific Instruments **86**, 024101 (2015); doi: 10.1063/1.4908196
View online: http://dx.doi.org/10.1063/1.4908196
View Table of Contents: http://scitation.aip.org/content/aip/journal/rsi/86/2?ver=pdfcov
Published by the AIP Publishing

Articles you may be interested in

Monodispersed magnetite nanoparticles optimized for magnetic fluid hyperthermia: Implications in biological systems
J. Appl. Phys. **109**, 07B310 (2011); 10.1063/1.3556948

Particle blocking and carrier fluid freezing effects on the magnetic properties of Fe 3 O 4 -based ferrofluids
J. Appl. Phys. **105**, 07B511 (2009); 10.1063/1.3068461

Macroscopic quantum tunneling of the magnetization in the single crystal of [(Mn 0.96 Cr 0.04) 12 O 12 (C H 3 C O O) 16 (H 2 O) 4] • 2 C H 3 C O O H • 4 H 2 O
Appl. Phys. Lett. **86**, 202509 (2005); 10.1063/1.1923752

Synthesis and complex magnetic susceptibility characterization of magnetic fluids in different liquid carriers
J. Appl. Phys. **97**, 10Q914 (2005); 10.1063/1.1854413

Effective magnetoviscosity of planar-Couette magnetic fluid flow
J. Appl. Phys. **97**, 10Q302 (2005); 10.1063/1.1850337

This article is copyrighted as indicated in the article. Reuse of AIP content is subject to the terms at: http://scitationnew.aip.org/termsconditions. Downloaded to IP: 128.179.253.15 On: Wed, 25 Feb 2015 16:18:20

A magnetic tunnel to shelter hyperpolarized fluids

Jonas Milani,[1,a)] Basile Vuichoud,[1] Aurélien Bornet,[1] Pascal Miéville,[1] Roger Mottier,[1] Sami Jannin,[1,2] and Geoffrey Bodenhausen[1,3,4,5]
[1]*Institut des Sciences et Ingénierie Chimiques, Ecole Polytechnique Fédérale de Lausanne (EPFL), Batochime, CH-1015 Lausanne, Switzerland*
[2]*Bruker BioSpin AG, Industriestrasse 26, CH-8117 Fällanden, Switzerland*
[3]*Département de Chimie, École Normale Supérieure-PSL Research University, 24 rue Lhomond, F-75005 Paris, France*
[4]*Sorbonne Universités, UPMC Univ Paris 06, LBM, 4 place Jussieu, F-75005 Paris, France*
[5]*CNRS, UMR 7203 LBM, F-75005 Paris, France*

(Received 26 September 2014; accepted 4 February 2015; published online 24 February 2015)

To shield solutions carrying hyperpolarized nuclear magnetization from rapid relaxation during transfer through low fields, the transfer duct can be threaded through an array of permanent magnets. The advantages are illustrated for solutions containing hyperpolarized ^{1}H and ^{13}C nuclei in a variety of molecules. © *2015 Author(s). All article content, except where otherwise noted, is licensed under a Creative Commons Attribution 3.0 Unported License.* [http://dx.doi.org/10.1063/1.4908196]

I. INTRODUCTION

Dynamic Nuclear Polarization (DNP)[1] provides an elegant way to overcome the lack of sensitivity in NMR since it can boost the nuclear spin polarization by several orders of magnitude. In dissolution-DNP (D-DNP),[2] one uses separate devices for polarization and detection. The polarizer operates at low temperatures and moderate magnetic fields (T = 1.2 K and B_0 = 6.7 T in our laboratory)[3–6] where the electron spin polarization can be close to unity, i.e., P(e) = 0.98 in our system. By suitable microwave irradiation, part of the electron spin polarization can be transferred to the nuclei of the frozen sample. A burst of hot solvent is then squirted onto the hyperpolarized sample so that it rapidly melts and approaches room temperature, at which point the hyperpolarization can beat Boltzmann's equilibrium polarization by four to five orders of magnitude. The sample is then transferred to a high-resolution NMR spectrometer or MRI scanner. The transfer of the hyperpolarized fluid from the polarizer to the detection magnet may cause dramatic losses of polarization since the magnetization decays through inexorable longitudinal "spin-lattice" relaxation with a field-dependent time constant T_1. Apart from a system based on a dual magnet[7] where the transfer can occur in less than a second, most polarizers are placed at a few meters distance from the NMR or MRI apparatus. The transfer times can therefore vary between a few seconds[8] and about a minute,[9] depending on the handling of the hyperpolarized fluid, which may pushed by a pressurized gas, carried manually, or filtered and neutralized. During the transfer, the hyperpolarized solution is no longer immersed in the magnetic field of the polarizer (typically between 3.35 and 6.7 T) and not yet sheltered by the field of the detection magnet (typically 1.5–18.6 T). During the transfer, the hyperpolarized sample may be exposed to very low magnetic fields (e.g., the Earth's magnetic field) or even to a vanishing field (e.g., if the two magnets have opposite polarity), depending on many parameters such as the design of the magnets (unshielded or actively shielded) and their relative orientations (fields pointing up or down). In field shuttling experiments, this low-field region has pertinently been referred to as "*death valley*."[10] The hyperpolarization is likely to perish in this hostile territory because various nuclear spin-lattice relaxation mechanisms may be exacerbated at low fields, including paramagnetic effects, scalar relaxation, etc.

In order to shield hyperpolarized solutions from such relaxation mechanisms, we have designed a modular "*magnetic tunnel*" to interface our home-built 6.7 T polarizer either to an unshielded 300 MHz or to an ultra-shielded 500 MHz high-resolution NMR spectrometer (see Fig. 1). We report in this work: (a) a map of the stray fields in our laboratory, (b) spin-lattice relaxation rates determined as a function of the magnetic field, (c) a discussion of the adiabatic condition that must be fulfilled during transfer, (d) details of the design of our magnetic tunnel, and (e) enhancement factors for an assortment of eight different solutions containing ^{1}H and ^{13}C spins in eleven different environments, transferred either with or without magnetic tunnel.

II. METHODS AND RESULTS

A. Magnetic field mapping

The stray magnetic fields in an NMR or MRI laboratory depend on many parameters. During a dissolution-DNP experiment, the hyperpolarized fluid must travel through the space between two magnets. The fate of the hyperpolarization depends on the strength and orientation of the stray fields. We have mapped the field between our polarizer and an unshielded 300 MHz NMR spectrometer using a triple-axis Hall probe (Sentron Digital 3D Teslameter, Type: 3MS1-A2-D3) using custom-designed National Instrument Labview software.

a)Author to whom correspondence should be addressed. Electronic mail: jonas.milani@epfl.ch. Tel.: +41 21 693 93 86.

 © Author(s) 2015

This article is copyrighted as indicated in the article. Reuse of AIP content is subject to the terms at: http://scitationnew.aip.org/termsconditions. Downloaded to IP: 128.179.253.15 On: Wed, 25 Feb 2015 16:18:20

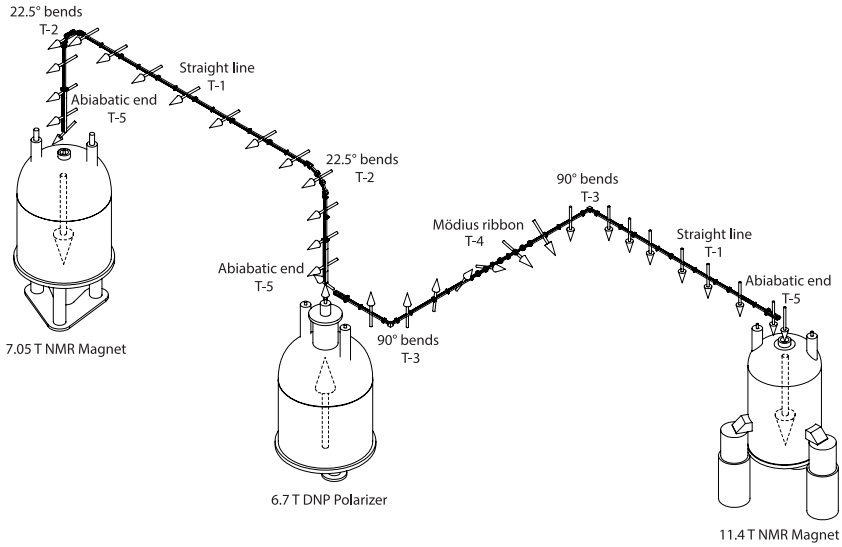

FIG. 1. Experimental arrangement in our laboratory consisting of a 6.7 T DNP polarizer (middle) coupled to an unshielded 300 MHz spectrometer (left) and to an ultra-shielded 500 MHz magnet (right), either through a "vertical" magnetic tunnel, i.e., with a vertical entrance and exit (left) or through a "horizontal" magnetic tunnel (right). The arrows that show the adiabatic changes of the direction of the magnetic field along the path are not drawn to scale. Since the two magnets on the right side have opposite static fields, the direction of the field is rotated adiabatically in a series of segments arranged in the manner of a Möbius ribbon. This is not necessary for the two magnets on the left side.

B. Relaxometry

Paramagnetic impurities affect the longitudinal relaxation of nuclei. This phenomenon is exploited in MRI by using contrast agents such as gadolinium complexes. But in our case, relaxation is undesirable, and losses of polarization during the transfer must be kept to a minimum. For DNP, we obviously need polarizing agents such as TEMPO, trityl, but their presence is no longer desirable after dissolution. With a custom-built shuttle relaxometer[11] operating in the stray field of an unshielded 300 MHz wide-bore Oxford Instruments magnet, we have studied the ^{1}H nuclear spin-lattice relaxation of bromothiophene carboxylate (BTC) (Sigma Aldrich) over a range 1 mT < B_0 < 7.05 T. The shuttle can lift the NMR sample with a stepper motor so that it reaches a field of 1 mT within *ca*. 1 s. Details about such measurements are given elsewhere.[11] Three samples were prepared, based on a 50 mM stock solution of bromothiophene carboxylate in non-degassed D_2O. Sample **1** without any additions, sample **2** with the addition of 0.25 mM 4-hydroxy-2,2,6,6-tetramethylpiperidine 1-oxyl (TEMPOL) (Sigma Aldrich), and sample **3** with the addition of 50 mM sodium ascorbate (Sigma Aldrich) which acts as scavenger that quenches both TEMPOL and dissolved O_2.[12] As discussed below, dissolution-DNP experiments are usually performed with frozen pellets containing 50 mM TEMPOL in addition to the analyte, with a typical volume 0.1 < v < 0.5 mL, and subsequently dissolved with 5 mL of hot D_2O or H_2O. The final TEMPOL concentration therefore usually ranges between 1 and 5 mM. In order to minimize relaxation during the relatively slow displacements of the shuttle, we decreased the TEMPOL concentration to 0.25 mM (4–20 times below the usual concentrations in routine dissolution-DNP experiments) so that the paramagnetic contribution to the relaxation rate is $R_1^{\text{para}} < 1\ \text{s}^{-1}$. The relaxation rates $R_1(^1\text{H})$ of bromothiophene carboxylate were measured in ten different magnetic fields B_0 = 7.05, 1.0, 0.4, 0.10, 0.022, 0.01, 0.004, 0.002, and 0.001 T. A single acquisition of the ^{1}H spectrum at 7 T sufficed for each data point.

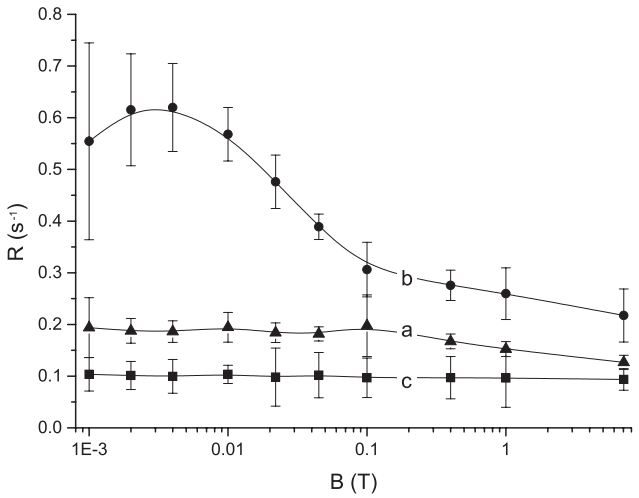

FIG. 2. Proton longitudinal ("spin-lattice") relaxation rates $R_1(^1\text{H}) = 1/T_1(^1\text{H})$ of bromothiophene carboxylate (BTC) (Sigma Aldrich) determined with a home-built relaxometer[11] as a function of the static field B_0 expressed on a logarithmic scale. (a) Triangles for sample 1 containing 50 mM BTC in D_2O with naturally dissolved O_2; (b) Dots for sample 2 after addition of 0.25 mM TEMPOL; (c) Squares for sample 3 after addition of 30 mM sodium ascorbate to scavenge radicals and paramagnetic oxygen.

Figure 2 shows the longitudinal relaxation rates $R_1(^1\text{H}) = 1/T_1(^1\text{H})$ in BTC. In sample **3**, where the paramagnetic oxygen has been scavenged by sodium ascorbate, $T_1(^1\text{H})$ is independent of the magnetic field down to 1 mT. However, samples **2** and **1** show a pronounced field-dependence, which can be attributed to the presence of paramagnetic dissolved oxygen and TEMPOL. One can distinguish three different contributions to relaxation: (1) a field-independent intra-molecular contribution $R_1^{\text{intra}} = 0.1 \pm 0.01\ \text{s}^{-1}$, (2) a field-dependent paramagnetic contribution due to dissolved

This article is copyrighted as indicated in the article. Reuse of AIP content is subject to the terms at: http://scitationnew.aip.org/termsconditions. Downloaded to IP: 128.179.253.15 On: Wed, 25 Feb 2015 16:18:20

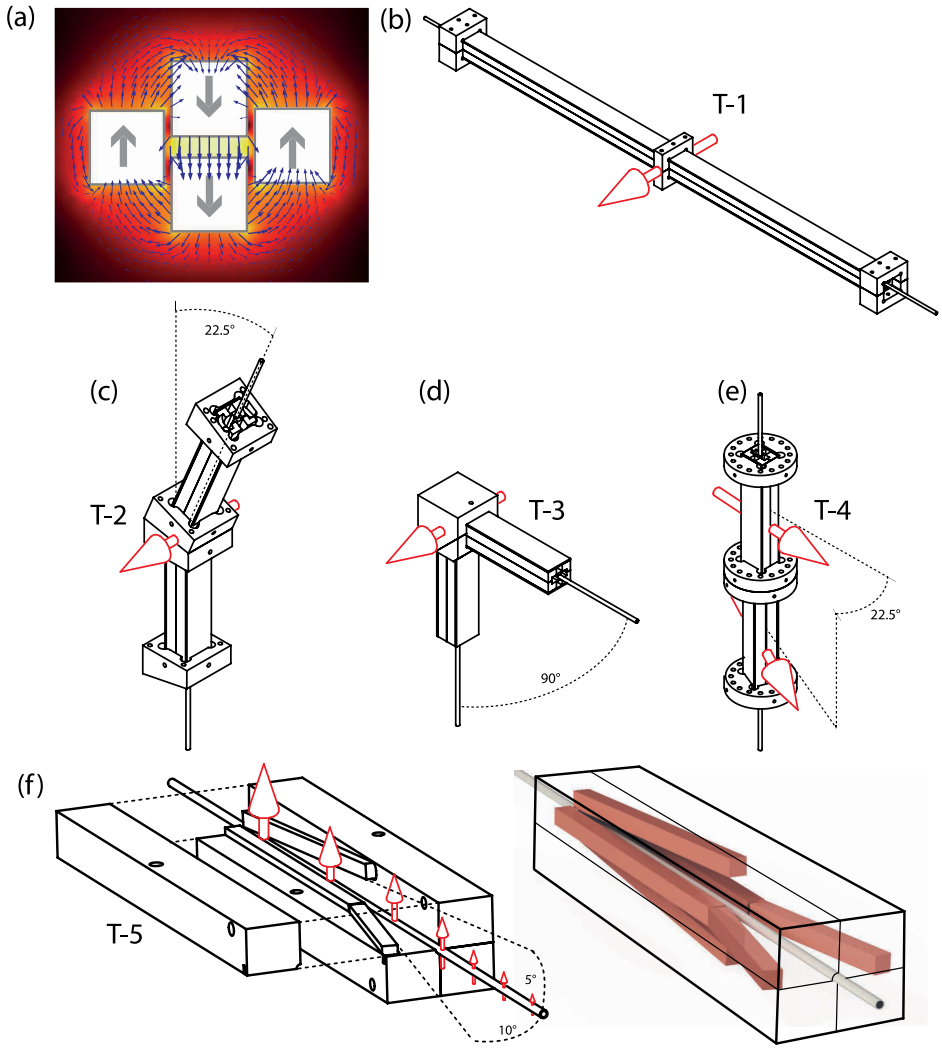

FIG. 3. (a) Simulations (Comsol Multiphysics) showing the magnetic field vectors in the magnetic tunnel where permanent magnets ($5\times5\times100$ mm, NdFeB) are positioned in four rows following a simplified Halbach design. The magnets are positioned to maximize the magnetic field strength in the center ($B_{\text{tunnel}} > 0.9$ T). A 2.5 mm outer diameter PTFE ("Teflon") tube carries the hyperpolarized fluid. Various magnetic tunnels can be assembled using four different modular segments: (b) linear segment of 50 cm length, (c) segment with 22.5° bend, (d) element with 90° bend, (e) segment with 22.5° axial twist, and (f) adiabatic section at entrance or exit of the tunnel where the magnets are positioned so as to diverge from the central tube. The left figure shows the aluminum support where one quarter has been removed to show the internal structure. The right figure shows the internal arrangement of the magnets. The red arrows show the direction of the field.

oxygen, increasing from $R_1^{\text{para}} = 0.08 \pm 0.01$ s^{-1} at $B_0 = 1$ T to $R_1^{\text{para}} = 0.1 \pm 0.01$ s^{-1} at 1 mT, and (3) a field-dependent paramagnetic contribution due to 0.25 mM TEMPOL increasing from $R_1^{\text{para}} = 0.1 \pm 0.05$ s^{-1} at $B_0 = 1$ T to $R_1^{\text{para}} = 0.4 \pm 0.05$ s^{-1} at 1 mT. For a more realistic TEMPOL concentration of 2 mM expected after dissolving 200 μl of frozen pellets with 5 ml of D_2O, this can be extrapolated to $R_1^{\text{para}} = 0.8 \pm 0.4$ s^{-1} at $B_0 = 1$ T and $R_1^{\text{para}} = 3.2 \pm 0.4$ s^{-1} at 1 mT.

This example is representative of the exacerbated relaxation at low magnetic fields during transfer in dissolution-DNP experiments. As a remedy to this detrimental effect, we have proposed the use of vitamin C (sodium ascorbate) as a scavenger[12] during dissolution, which turned out to be a useful approach when hyperpolarizing nuclei with long T_1 such as ^{13}C. However, this scavenging process may take several seconds to complete, an interval during which paramagnetic relaxation is still active and drives the hyperpolarization back towards thermal equilibrium. Obviously, as illustrated in Fig. 2 for the case of ^{1}H spins in BTC, and more generally for protons in small molecules, the interval where hyperpolarized molecules are exposed to the effects of concentrated radicals at low magnetic field cause painful losses of priceless polarization.

C. Magnetic tunnel

Our magnetic tunnel consists of an assembly of permanent neodymium boron magnets (Supermagnete Webcraft GmbH, $5\times5\times100$ mm, NdFeB, N52, with Ni-Cu-Ni coating) securely maintained by several home-built aluminum structures. The permanent magnets are positioned in four rows following a simplified Halbach design[13] and oriented to maximize the magnetic field strength in the center, where $B_{\text{tunnel}} > 0.9$ T (see Fig. 3(a)). A hollow cylinder with a 3 mm inner diameter runs through the center of the aluminum structure to guide a 2.5 mm outer diameter polytetrafluoroethylene (PTFE) ("Teflon") tube (Maagtechnic

This article is copyrighted as indicated in the article. Reuse of AIP content is subject to the terms at: http://scitationnew.aip.org/termsconditions. Downloaded to IP: 128.179.253.15 On: Wed, 25 Feb 2015 16:18:20

AG 10075652) that carries the hyperpolarized fluid. The design comprises five different modular segments T-1–T-5: straight sections of 50 cm length (T-1, see Fig. 3(b)), bending sections with an angle of 22.5° (T-2, see Fig. 3(c)) or 90° (T-3, see Fig. 3(d)) where the magnetic field is perpendicular to the plane of the bend, so that the field vectors remain parallel. The choice between a single 90° bend and a series of 22.5° bends depends on the constraints of the laboratory. Special attention must be paid to variations of the magnetic field at the entrance and exit of the tunnel. The adiabatic condition (*vide infra*) must be fulfilled throughout, and zero-field crossings should be avoided, in particular at the entry and exit of the tunnel. In order to avoid zero-field crossings when the stray fields have opposite orientations (as for our DNP polarizer and NMR magnets), we have designed an 22.5° axial twist section of 10 cm length (T-4, see Fig. 3(e)). A cascade of eight axial twist sections allows one to achieve a 180° rotation of the field, in the manner of a Möbius ribbon (see Fig. 1). Without 180° rotation, the magnetic field would inevitably cross through zero at one of the ends of the tunnel. Finally, we have designed a tunnel section (T-5, see Fig. 3(f)) where the magnetic field is gradually increased from 0 to 0.9 T, so as to fulfill the adiabatic condition even if the sample is transferred very rapidly at a velocity of, say, 10 ms^{-1}. These segments can be assembled in a flexible way to accommodate the dimensions of individual laboratories.

D. Adiabatic condition

The main purpose of the magnetic tunnel is to prevent losses of polarization at low fields, by providing a minimum field ($B_{tunnel} > 0.9$ T) that is sufficient to sustain the hyperpolarization during transfer. However, a sudden change of the direction of the magnetic field may cause a loss of magnetization if the rate of change is comparable to the Larmor frequency. Therefore, particular care has been taken to design the entrance and exit of the tunnel where the magnetic field may change abruptly. The T-5 segment (see Fig. 2(f)) offers a way to increase or decrease the magnetic field in such a way that the following condition of adiabaticity is always fulfilled:[14]

$$\frac{1}{B^2}\left|\vec{B}\times\frac{d\vec{B}}{dt}\right| \ll \gamma B, \tag{1}$$

where $B = \left|\overrightarrow{B_{stray}} + \overrightarrow{B_{tunnel}}\right|$ is the total magnetic field. The Larmor frequency is $\gamma B/(2\pi) = 4.26$ kHz for protons if $B = 100$ μT. The adiabatic condition is obviously more critical for low-gamma nuclei such as carbon-13 or nitrogen-15 that are popular for dissolution DNP. We define a dimensionless adiabatic ratio

$$A = \left|\vec{B}\times\frac{d\vec{B}}{dt}\right|/\gamma B^3 \tag{2}$$

which should be kept as small as possible, preferably $A < 1$. Note that A is proportional to the speed of the transfer of the sample through the PTFE tube. Figure 4 illustrates how the entrance and exit of the magnetic tunnel raises delicate issues that can be solved by inserting an adiabatic T-5 section.

Figure 4(b) shows the magnetic field profile (red line) at the entrance of a straight T-1 section. The first striking feature is that, just before the entrance, the magnetic field has a sign that is opposite ($B_{out} = -60$ μT) to the magnetic field inside the section ($B_{tunnel} > +0.9$ T). A hyperpolarized sample entering into such a straight T-1 section therefore inevitably undergoes a detrimental zero-field crossing. This does not matter if the entrance of the tunnel is placed in a stray field of a superconducting magnet $B_{stray} > B_{out}$, provided that B_{stray} is not anti-parallel to B_{tunnel}. A second striking feature of Fig. 4(b) is the sudden increase in magnetic field at the entrance. The magnetic field increases to $B_{tunnel} > +0.9$ T in a quasi-instantaneous manner. Unless the magnetic field outside the tunnel $B_{out} + B_{stray}$ is parallel to B_{tunnel}, such an abrupt change in the strength of the magnetic field will be accompanied by a sudden change in its direction. Figure 4 also shows (red lines) the adiabatic factor A of Eq. (2) calculated for a scenario where B_{stray} is perpendicular to B_{tunnel}. We show in Fig. 4(a) that both issues of zero-field crossings and abrupt field changes can be overcome by using an adiabatic T-5 section rather than a simple straight T-1 section. In this example, $A \sim 10^{-3}$. Unfortunately, as shown in Fig. 1, the DNP polarizer (Oxford Instruments) has a polarity opposite to both 300 and 500 MHz NMR spectrometers (Bruker BioSpin). For the 300 spectrometer, we used a "vertical" tunnel (see Fig. 1) where B_{stray} and B_{tunnel} are perpendicular so that no zero-crossings occur. For the 500 MHz NMR spectrometer, space restrictions forced us to use a "horizontal" configuration. If B_{stray} and B_{tunnel} are anti-parallel, the only way to avoid a zero-field crossing is to reverse the direction of B_{tunnel}. This

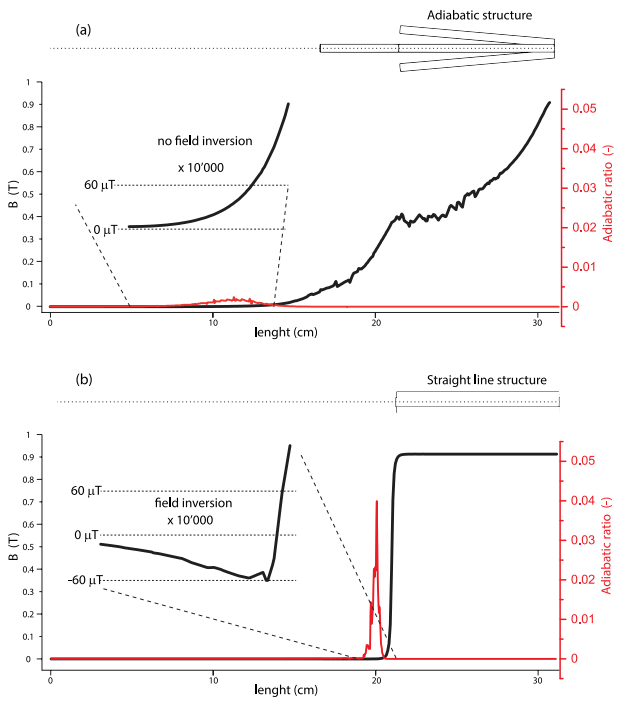

FIG. 4. Simulations of the magnetic field (black lines) and of the adiabatic ratio A of Eq. (2) (red lines) at the entrance or exit of the magnetic tunnel for (a) an adiabatic section (see Fig. 3(f)) and (b) a straight section (see Fig. 3(b)). The adiabatic ratio A, which must be smaller than 1, is proportional to the speed of the sample transfer. It is shown here for a realistic speed of 10 m/s.

This article is copyrighted as indicated in the article. Reuse of AIP content is subject to the terms at: http://scitationnew.aip.org/termsconditions. Downloaded to IP: 128.179.253.15 On: Wed, 25 Feb 2015 16:18:20

was achieved by inserting eight 22.5° axial twist sections (T-4) to rotate the magnetic field through 180°, so as to match the opposite orientations of the stray fields at the two ends of the tunnel.

E. Dissolution-DNP experiments

Three DNP solutions were prepared to test the advantages of the magnetic tunnel for dissolution-DNP experiments. Solution **4** contained 1 M BTC (Sigma Aldrich) and 50 mM TEMPOL in DMSO-d_6/D_2O (60/40 **v:v**). Solution **5** contained 1 M alanine-glycine (Sigma Aldrich) and 50 mM TEMPOL in ethanol-d_6/D_2O (50/50 **v:v**), and solution **6** contained 3 M ^{13}C-labeled urea and 50 mM TEMPOL in DMSO-d_6/D_2O (60/40 **v:v**). The DNP solutions were rapidly frozen to form 10 μl pellets in liquid nitrogen, and 20 pellets (total sample volume of 200 μl) were loaded in the cryostat of our 6.7 T polarizer that was pre-cooled to T = 4.2 K. The cryostat was further cooled down to T = 1.2 K and microwave irradiation was applied during 20 min with an input power $P_{\mu w}$ = 87 mW at a monochromatic irradiation frequency $f_{\mu w}$ = 188.3 GHz to induce the strongest possible (negative) proton polarization. The proton DNP build-up curves were measured at T = 2.2 K and B_0 = 6.7 T with 5° pulses applied every 5 s. Dissolution was subsequently performed with 5 mL D_2O preheated to *ca.* T = 450 K at a pressure of 1 MPa. The hyperpolarized liquid bolus was propelled with helium gas at 0.6 MPa to either 300 or 500 MHz spectrometers, both at a distance of *ca.* 5 m. Two distinct PTFE ("Teflon") transfer tubes, both with 1.5 inner diameters, were used: one running through one of the magnetic tunnels, the other running loosely between the polarizer and either of the two spectrometers. After settling for *ca.* 2 s, the sample was injected into 5 mm NMR tubes using home-built injection devices. The typical intervals in this sequence are dissolution in 0.7 s, transfer in 5 s, and injection in 2.5 s. The decay of the ^{1}H NMR signal was measured every 5 s with 5° pulses.

III. RESULTS AND DISCUSSION

The field along the magnetic tunnel depends on the configuration of the superconducting magnets and their shielding. The graph in Fig. 5 shows the magnitude of the magnetic field (without magnetic tunnel) in the plane between our DNP polarizer (unshielded 6.7 T magnet) and our 300 MHz NMR spectrometer (unshielded 7.05 T magnet). Even though the two magnets are unshielded in this example, the magnetic field drops below B_0 = 1 mT. A similar measurement between our polarizer and ultra-shielded 500 MHz magnet (not shown in Fig. 5) indicates that the field drops as low as B_0 < 0.5 mT.

In order to study the detrimental effects of increased relaxation at low field during transfer, we have performed dissolution-DNP experiments with solutions **4** and **5** containing ^{1}H spins in an assortment of molecules, with and without magnetic tunnel. In all cases, the polarization process yielded a nuclear spin polarization $P(^1H)$ > 60% with a typical build-up time constant τ_{DNP} = 280 ± 10 s. The advantage of a transfer through a magnetic tunnel, compared to a transfer through a low field region, can be expressed in terms of an enhancement factor $\varepsilon_{tunnel}(^1H)$ or $\varepsilon_{tunnel}(^{13}C)$. Figures 6 and 7 show ^{1}H and ^{13}C spectra and molecular structures of various hyperpolarized molecules in solutions **4**, **5**, and **6**, obtained with and without magnetic tunnel. The spin-lattice relaxation times $T_1(^1H)$ or $T_1(^{13}C)$ measured in high field and the tunnel enhancement factors $\varepsilon_{tunnel}(^1H)$ or $\varepsilon_{tunnel}(^{13}C)$ are reported in Tables I and II.

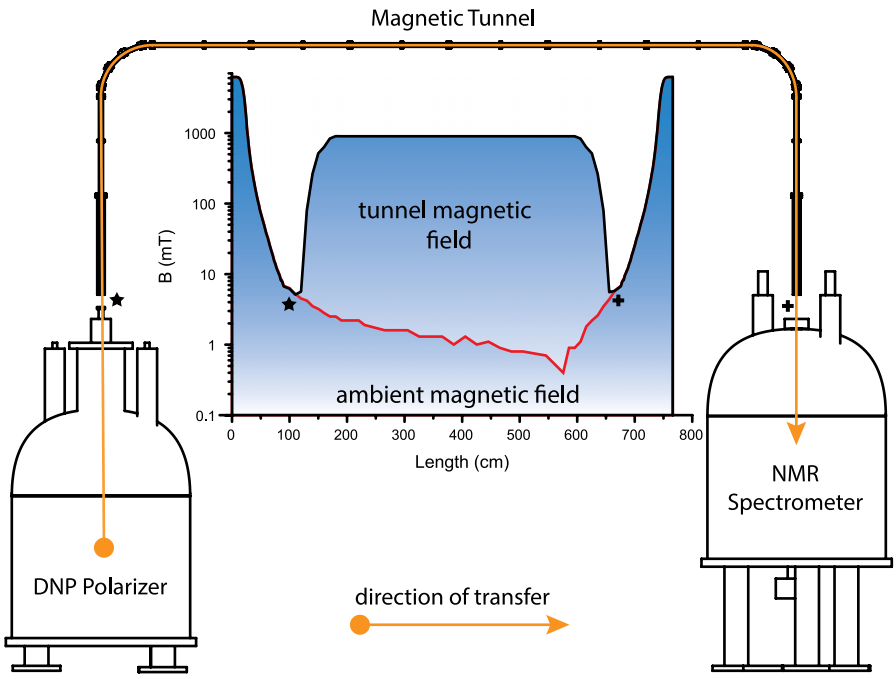

FIG. 5. The magnetic field strength in the course of the transfer of the hyperpolarized fluid from the DNP polarizer to the unshielded 300 MHz NMR spectrometer through a magnetic tunnel (black line) or without tunnel (red line). The star and cross indicate the polarizer-tunnel and tunnel-spectrometer junctions. Details of the orientation of the magnetic fields at the entrance and exit of the tunnel are shown in Fig. 1.

This article is copyrighted as indicated in the article. Reuse of AIP content is subject to the terms at: http://scitationnew.aip.org/termsconditions. Downloaded to IP: 128.179.253.15 On: Wed, 25 Feb 2015 16:18:20

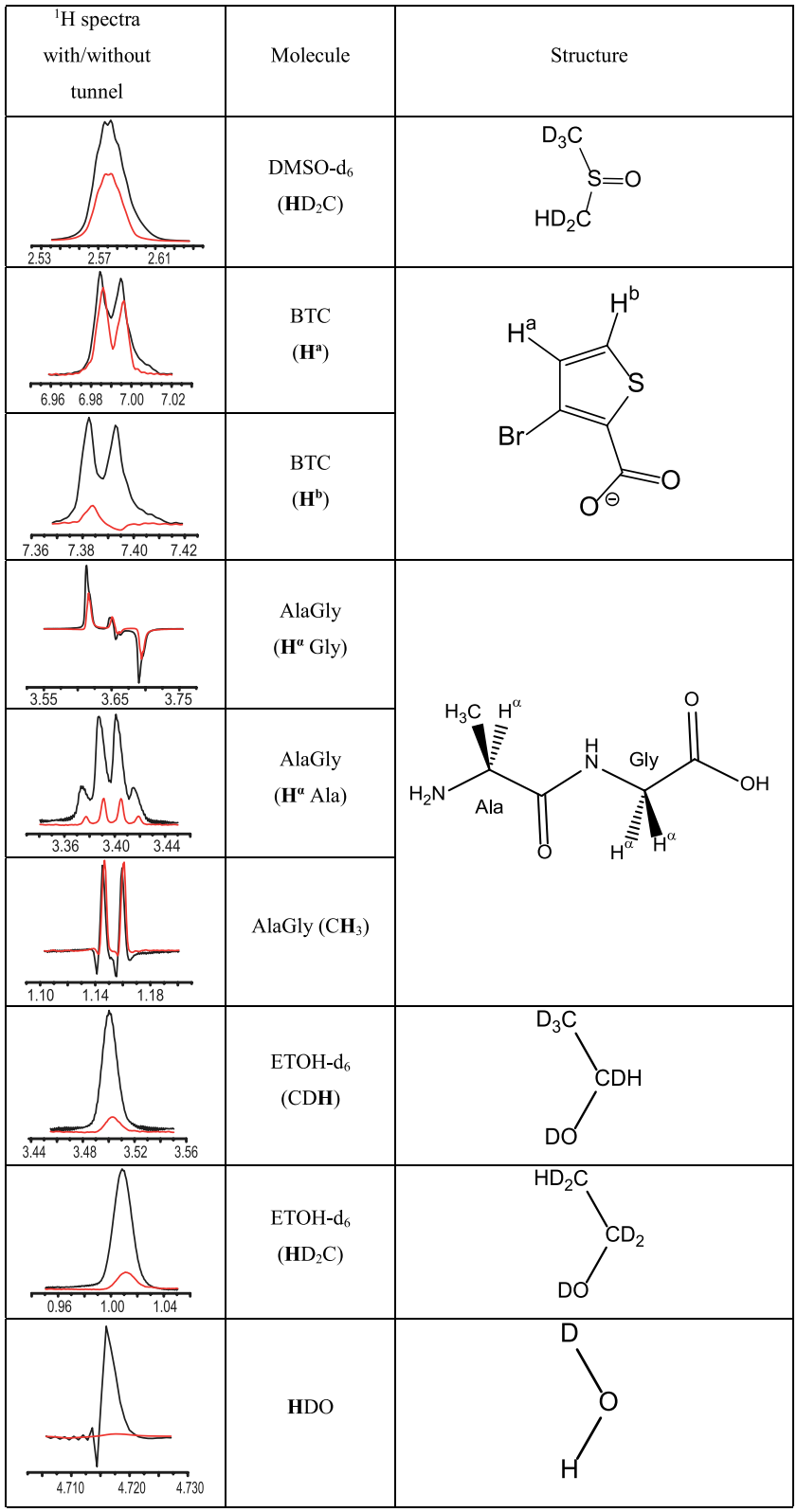

FIG. 6. Proton NMR spectra obtained after hyperpolarization and dissolution with and without magnetic tunnel, shown in black and red, respectively.

Surprisingly enough, the enhancement factors vary significantly from case to case, with two extreme examples of the fully protonated methyl group of AlaGly with $\varepsilon_{tunnel}(^1H) = 1.0$ and the residual protons in 99.9% deuterated water with $\varepsilon_{tunnel}(^1H) = 25.3$ (Table I). These two examples are instructive and can be readily understood. The relaxation of the fully protonated methyl group of AlaGly is not significantly affected by the presence of free radicals since relaxation through intrinsic ^{1}H-^{1}H dipolar interactions is dominant. On the other hand, the residual protons in HDO mainly relax though paramagnetic interactions with dissolved oxygen and TEMPOL. Indeed, when TEMPOL and oxygen are scavenged

This article is copyrighted as indicated in the article. Reuse of AIP content is subject to the terms at: http://scitationnew.aip.org/termsconditions. Downloaded to IP: 128.179.253.15 On: Wed, 25 Feb 2015 16:18:20

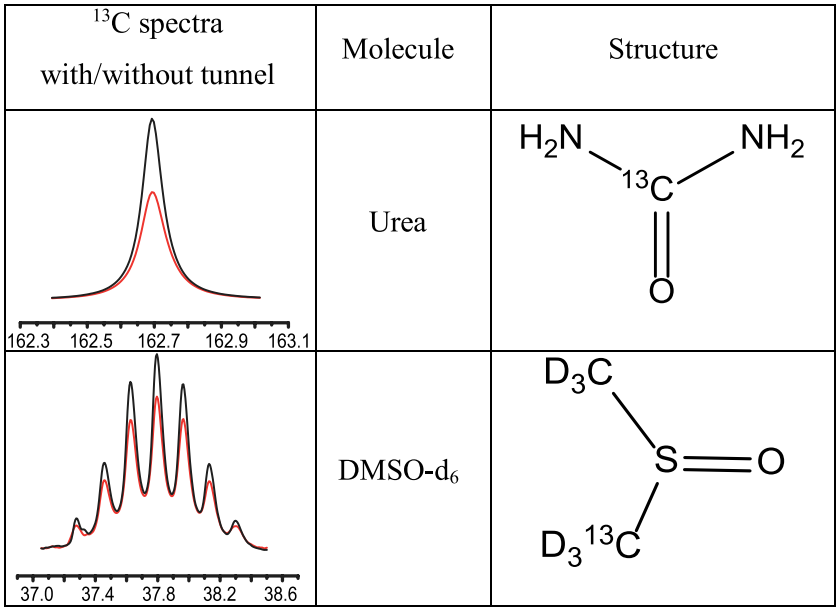

FIG. 7. ^{13}C NMR spectra obtained after hyperpolarization and dissolution with and without magnetic tunnel (black and red lines, respectively).

by vitamin C, the spin-lattice relaxation time in HDO increases from $T_1(^1\text{H})$ from 3.6 to 14 s at 7 T. As an alternative to scavenging, we have shown recently that paramagnetic relaxation can also be prevented by replacing the soluble TEMPOL by hybrid polarizing solids (HYPSO) that can be eliminated by on-line filtration during the dissolution process.[15]

It is therefore natural that hyperpolarization losses during transfer are strongly attenuated by using a magnetic tunnel in the case of HDO, but not in the case of CH_3. A more detailed analysis could be performed from case to case, with a full calculation of paramagnetic relaxation which would depend on a myriad of parameters such as (**1**) the distance d of closest electron-proton approach and (**2**) the mutual electron-proton translational diffusion constant D which is specific for each system, (**3**) the magnetic field along the transfer, and the (**4**) the speed of the transfer. The results for ^{13}C nuclei reported in Table II are far less impressive in terms of enhancements, with $\varepsilon_{\text{tunnel}}(^{13}\text{C}) \leq 1.3$. This can be explained by the ^{13}C nuclear spin-lattice relaxation times that tend to be longer than the transfer times, even at low magnetic fields. It is worth stressing that for extended transfer times (for example, when hyperpolarized fluids must be manipulated for filtration, in fairly low magnetic fields) relaxation effects can become significant even for ^{13}C, as recently reported by Chiavazza *et al.*[16] The general trend arising from Table I is that for isolated ^{1}H spins as well as for pairs of equivalent ^{1}H spins, the use of our magnetic tunnel can be recommended. However, there are some cases that deserve further investigation: (1) the H^α of the Gly residue in AlaGly benefits from the use of the magnetic tunnel since $\varepsilon_{\text{tunnel}}(^1\text{H}) = 1.8$, but its antiphase pattern (which suggests an admixture of I_z and $2I_zS_z$ terms) has not been rationalized so far; (2) the signal of H^b in BTC was almost completely wiped out when the magnetic tunnel is not used (hence, the favorable ratio $\varepsilon_{\text{tunnel}}(^1\text{H}) > 12$), whereas the signal of H^a merely suffered moderate losses in the absence of magnetic tunnel ($\varepsilon_{\text{tunnel}}(^1\text{H}) = 1.5$). Previous studies suggest that these effects could be due to scalar couplings with quadrupolar nuclei at low field,[16] in this example bromine or nitrogen-14. Such scalar relaxation effects can be attenuated by using our magnetic tunnel. Another interesting way to make hyperpolarization immune to very low fields, so that there would be no need for a magnetic tunnel, is to store the polarization in the form of "equivalent hyperpolarized long-lived states" (HELLS).[17] However, these approaches are limited to analytes that fulfill demanding conditions of molecular symmetry. The use of magnetic tunnels appears to offer a more universal solution at the time of writing.

IV. CONCLUSIONS

We have demonstrated that the hyperpolarization of protons can be better preserved in dissolution-DNP by using magnetic tunnels. The benefits have been illustrated by several examples with improvement factors ranging between $1 < \varepsilon_{\text{tunnel}} < 25$ for protons and carbon-13 nuclei.

TABLE I. Longitudinal relaxation times $T_1(^1\text{H})$ and enhancement factors $\varepsilon_{\text{tunnel}}(^1\text{H})$ measured after hyperpolarization and dissolution at room temperature at 500 MHz ($B_0 = 11.7$ T) in solutions containing approximately 2 mM TEMPOL. BTC stands for bromothiophene carboxylate.

Molecule	DMSO-d_6 ($\mathbf{H}D_2C$)	BTC ($\mathbf{H}^a$)	BTC ($\mathbf{H}^b$)	AlaGly ($\mathbf{H}^\alpha$ Gly)	AlaGly ($\mathbf{H}^\alpha$ Ala)	AlaGly ($C\mathbf{H}_3$)	ETOH-d_6 ($CD\mathbf{H}$)	ETOH-d_6 ($\mathbf{H}D_2C$)	**H**DO
T_1 (^{1}H) (s)	13.2 ± 0.02	5.7 ± 0.1	6.0 ± 0.1	6.0 ± 0.1	4.1 ± 1.4	...	4.0 ± 0.4	4.3 ± 0.3	3.6 ± 0.1
$\varepsilon_{\text{tunnel}}(^1\text{H})$	2.1	1.5	12.2	1.8	9.0	1.0	10.2	8.6	25.3

This article is copyrighted as indicated in the article. Reuse of AIP content is subject to the terms at: http://scitationnew.aip.org/termsconditions. Downloaded to IP: 128.179.253.15 On: Wed, 25 Feb 2015 16:18:20

TABLE II. Longitudinal relaxation times $T_1(^{13}C)$ and enhancement factors $\varepsilon_{tunnel}(^{13}C)$ measured after hyperpolarization and dissolution at room temperature at 500 MHz ($B_0 = 11.7$ T) in solutions containing approximately 2 mM TEMPOL.

Molecule	Urea	DMSO-d_6
T_1 (^{13}C) (s)	31.5 ± 1.9	26.9 ± 1.4
$\varepsilon_{tunnel}(^{13}C)$	1.3	1.2

The enhancement factors depend on many parameters and vary greatly from one nucleus to another, from one molecule to another, and most probably from one laboratory to another. However, we have never witnessed any detrimental effects of our magnetic tunnels.

ACKNOWLEDGMENTS

The authors thank Martial Rey and Anto Barisic for valuable assistance. This work was supported by the Swiss National Science Foundation (SNSF), the Ecole Polytechnique Fédérale de Lausanne (EPFL), the Swiss Commission for Technology and Innovation (CTI), Bruker BioSpin Switzerland AG, the French CNRS, and the European Research Council (ERC Contract No. 339754 "Dilute para-water").

[1]A. Abragam and M. Goldman, Rep. Prog. Phys. **41**, 395 (1978).
[2]J. H. Ardenkjaer-Larsen, B. Fridlund, A. Gram, G. Hansson, L. Hansson, M. H. Lerche, R. Servin, M. Thaning, and K. Golman, Proc. Natl. Acad. Sci. U.S.A. **100**, 10158 (2003).
[3]A. Comment, B. van den Brandt, K. Uffmann, F. Kurdzesau, S. Jannin, J. A. Konter, P. Hautle, W. T. H. Wenckebach, R. Gruetter, and J. J. van der Klink, Concepts Magn. Reson., Part B **31B**, 255 (2007).
[4]A. Comment, B. van den Brandt, K. Uffmann, F. Kurdzesau, S. Jannin, J. A. Konter, P. Hautle, W. T. Wenckebach, R. Gruetter, and J. J. van der Klink, Appl. Magn. Reson. **34**, 313 (2008).
[5]S. Jannin, A. Comment, F. Kurdzesau, J. A. Konter, P. Hautle, B. van den Brandt, and J. J. van der Klink, J. Chem. Phys. **128**, 241102 (2008).
[6]S. Jannin, A. Bornet, R. Melzi, and G. Bodenhausen, Chem. Phys. Lett. **549**, 99 (2012).
[7]J. Leggett, R. Hunter, J. Granwehr, R. Panek, A. J. Perez-Linde, A. J. Horsewill, J. McMaster, G. Smith, and W. Kockenberger, Phys. Chem. Chem. Phys. **12**, 5883 (2010).
[8]S. Bowen and C. Hilty, Phys. Chem. Chem. Phys. **12**, 5766 (2010).
[9]S. J. Nelson, D. Vigneron, J. Kurhanewicz, A. Chen, R. Bok, and R. Hurd, Appl. Magn. Reson. **34**, 533 (2008).
[10]M. Reese, D. Lennartz, T. Marquardsen, P. Hofer, A. Tavernier, P. Carl, T. Schippmann, M. Bennati, T. Carlomagno, F. Engelke, and C. Griesinger, Appl. Magn. Reson. **34**, 301 (2008).
[11]P. Mieville, S. Jannin, and G. Bodenhausen, J. Magn. Reson. **210**, 137 (2011).
[12]P. Mieville, P. Ahuja, R. Sarkar, S. Jannin, P. R. Vasos, S. Gerber-Lemaire, M. Mishkovsky, A. Comment, R. Gruetter, O. Ouari, P. Tordo, and G. Bodenhausen, Angew. Chem., Int. Ed. **49**, 6182 (2010).
[13]K. Halbach, Nucl. Instrum. Methods **169**, 1 (1980).
[14]B. F. Melton, V. L. Pollak, T. W. Mayes, and B. L. Willis, J. Magn. Reson., Ser. A **117**, 164 (1995).
[15]D. Gajan, A. Bornet, B. Vuichoud, J. Milani, R. Melzi, H. A. van Kalkeren, L. Veyre, C. Thieuleux, M. P. Conley, W. R. Gruning, M. Schwarzwalder, A. Lesage, C. Coperet, G. Bodenhausen, L. Emsley, and S. Jannin, Proc. Natl. Acad. Sci. U. S. A. **111**, 14693 (2014).
[16]E. Chiavazza, E. Kubala, C. V. Gringeri, S. Duwel, M. Durst, R. F. Schulte, and M. I. Menzel, J. Magn. Reson. **227**, 35 (2013).
[17]A. Bornet, X. Ji, D. Mammoli, B. Vuichoud, J. Milani, G. Bodenhausen, and S. Jannin, Chem. - Eur. J. **20**, 17113 (2014).

This article is copyrighted as indicated in the article. Reuse of AIP content is subject to the terms at: http://scitationnew.aip.org/termsconditions. Downloaded to IP: 128.179.253.15 On: Wed, 25 Feb 2015 16:18:20